EFDA–JET–PR(11)41

T. Hellsten, T. Johnson, D. Van Eester, E. Lerche, Y. Lin, M.-L. Mayoral,
J. Ongena, G. Calabro, K. Crombé, D. Frigione, C. Giroud, M. Lennholm,
P. Mantica, M.F.F. Nave, V. Naulin, C. Sozzi, W. Studholme, T. Tala,
T. Versloot and JET EFDA contributors

On Rotation in Plasmas with Electron Heating by ICRH

On Rotation in Plasmas with Electron Heating by ICRH

T. Hellsten[1], T. Johnson[1], D. Van Eester[2], E. Lerche[2], Y. Lin[4], M.-L. Mayoral[3], J. Ongena[2], G. Calabro[9], K. Crombé[2], D. Frigione[9], C. Giroud[3], M. Lennholm[3], P. Mantica[5], M.F.F. Nave[6], V. Naulin[8], C. Sozzi[9], W. Studholme[3], T. Tala[7], T. Versloot[10] and JET EFDA contributors*

JET-EFDA, Culham Science Centre, OX14 3DB, Abingdon, UK

[1]EURATOM-VR Association, EES, KTH, Stockholm, Sweden
[2]LPP-ERM/KMS, Association Euratom-Belgian State, 1000 Brussels, Belgium, TEC Partner
[3]EURATOM-CCFE Fusion Association, Culham Science Centre, OX14 3DB, Abingdon, OXON, UK
[4]Plasma Science and Fusion Centre, MIT, Cambridge, USA
[5]Instituto di Fisica del Plasma, EURATOM-ENEA-CNR Association, Milan, Italy
[6]EURATOM/IST Fusion Association, Instituto de Plasmas e Fusão Nuclear, Instituto Superior Technico, Universidade Technica de Lisboa, Portugal
[7]HUT, Association EURATOM-Tekes, Finland
[8]Association EURATOM-Risø, National Laboratory, Denmark
[9]EURATOM-ENEA sulla Fusione, C. R. Frascati, Frascati, Italy
[10] FOM Institute for Plasma Physics Rijnhuizen, Association EURATOM-FOM, The Netherlands, TEC Partner
** See annex of F. Romanelli et al, "Overview of JET Results", (23rd IAEA Fusion Energy Conference, Daejon, Republic of Korea (2010)).*

Preprint of Paper to be submitted for publication in
Plasma Physics and Controlled Fusion

ABSTRACT

Rotation of L-mode plasmas in the JET tokamak heated by waves in the Ion Cyclotron Range of Frequencies (ICRF) damped on electrons is reported. The plasma is found to rotate in the counter current direction in the core with high shear. The rotation is stronger in magnitude than observed for scenarios with dominating ion cyclotron absorption. Two scenarios are considered: the inverted mode conversion scenarios and heating at the second harmonic ^{3}He cyclotron resonance in H-plasmas. In the latter case electron absorption of the fast magnetosonic wave by Transit Time Magnetic Pumping and Electron Landau Damping (TTMP/ELD) is the dominating absorption mechanism. Inverted mode conversion is done in (^{3}He)-H plasmas where the mode converted waves are essentially absorbed by electron Landau damping. Similar rotation profiles are seen when heating at the second harmonic cyclotron frequency of ^{3}He and with mode conversion at high concentrations of ^{3}He. The magnitude of the counter rotation is found to decrease with increasing plasma current. The correlation of the rotation with the electron temperature is better than with coupled power indicating that for these types of discharges the dominating mechanism for the rotation is related to indirect effects of electron heat transport rather than to direct effects of ICRF-heating.

1. INTRODUCTION

Rotation of plasmas is considered to be beneficial for confinement and stability by suppressing drift waves and resistive wall modes. The main source for driving rotation in present day experiments is neutral beam injection. However, the momentum input by neutral beam injection in ITER and future thermonuclear reactors will be rather low due the high density and large volume of ITER plasmas rendering the penetration of the beams into the core of the plasma difficult. It is therefore of interest to investigate alternative methods to generate rotation. Toroidal rotation of the plasma is often seen during Ion Cyclotron Resonance Heating (ICRH) even when the momentum inputs by the waves are negligible [1-14]. In general, the rotation is rather small and caused by several weak mechanisms that are not fully understood. Some of them are specific to the heating method caused by absorption of the momentum of the waves used for heating or by finite drift orbit effects of energetic ions produced by heating. Others are caused by changes in the plasma temperature, and are not specific to the heating method (intrinsic rotation). Some effects have been experimentally confirmed, but there still remain other observations that need to be explained. The strongest observed counter rotation with ICRH alone in JET is obtained with strong magnetic field ripple $\delta = (B_{max}-B_{min})/(B_{max}+B_{min}) \sim 1.5\%$ [9], where B_{max} and B_{min} are the maximum and minimum field at the plasma boundary at the outer midplane. Plasma rotation has also been observed during ohmic heating [10] and in experiments using waves in the Electron Cyclotron Range of Frequencies (ECRF) [8]. The main differences between ICRF and ECRF are: (i) the ratio between momentum and energy densities for ECRF waves is smaller than for ICRF (ion cyclotron range of frequencies) waves; and (ii) ECRF waves are directly absorbed on electrons. The rotation profiles of ECRH and ohmic heated plasmas are characterized by centrally peaked counter rotating profiles. In TCV it was observed that the peaked rotation profiles during ECRH were flattened by sawtooth crashes [8].

Various mechanisms have been identified to give rise to torques, for which the estimated rotation profiles caused by the torque are comparable to that observed in experiments. The momentum input by directed waves has been predicted to affect the rotation, and evidence of this has been obtained previously by comparing plasmas heated with fast magnetosonic waves propagating in the co and the counter current directions with modelling [15]; the absorbed wave momentum and the change in toroidal rotation was in agreement with simulations with the SELFO code [16, 17]. However, there are changes in the rotation profiles that cannot adequately be modelled with existing heating codes. As ions are heated from thermal to supra thermal energies, finite orbit width effects can give rise to rotation. In recent experiments, with H-minority heating in deuterium plasmas, it was shown that the torque caused by these supra thermal ions was not sufficient to fully explain the rotation; assuming that the momentum confinement was similar to the energy confinement time, the rotation resulting from the finite orbit effect was about a factor of three too low [3]. In a spatial dispersive medium, the change in the momentum of the waves by non-resonant interactions as the waves propagate across the plasma, can give rise to a torque in the plasma [18, 19]. As the wave is absorbed, the momentum is transferred to the plasma. This change in momentum by non-resonant interactions results in a torque on the plasma with a dipolar character and adds to the torque from the momentum the wave had when it was launched at the antenna. The change in momentum is, in particular, important for slow waves like those obtained by mode conversion of the fast magnetosonic wave, and could therefore result in large torques on the plasma in mode conversion experiments. Emission and absorption of drift waves, causing anomalous transport can in a similar way give rise to dipolar like torques due to the universal nature of the momentum and energy changes in wave-particle interactions.

The launched fast magnetosonic ICRF waves can be absorbed by ions and electrons either directly or indirectly through mode conversion to slow waves. Ion cyclotron damping at lower harmonics is often the dominating damping process of ICRH. If the power density is high, high-energy tails develop in the resonant ion distribution functions, and a large fraction of the power absorbed by ions will then be transferred to the electrons. High-energy ions with broad orbits, created by ICRH, can give rise to radial currents driving rotation. Most of the earlier rotation studies on JET [3, 9] with ICRH were done in scenarios with dominating ion cyclotron resonance absorption, where the power was transferred to ions and electrons by collisions. Few studies were done with direct electron absorption of the fast magnetosonic waves by Transit Time Magnetic Pumping and Electron Landau Damping (TTMP/ELD), which in current experiments is often a weak damping mechanism. Another way to heat electrons without first heating ions is to convert the magnetosonic waves into slow kinetic waves damped by ELD or ion cyclotron absorption. The electron damping of the mode converted wave is usually strong, and dominates the absorption above a certain minority concentration. It is usually more localised than the power deposition by direct absorption of the fast magnetosonic wave by TTMP/ELD.

Most rotation studies in JET have been done in ohmically heated and L-mode plasmas. Typical rotation profiles observed during H minority central ICRF heating in the absence of strong field

ripple (δ <0.08%) in JET show a positive rotation (i.e. in the direction of the plasma current) for most of the plasma radius with little shear in the outer part of the plasma. In the core, rotation can nevertheless be positive or negative [3] depending on the plasma current. For low plasma currents the rotation profiles are often hollow in the centre; in some cases even with negative rotation in the plasma centre. On the contrary, for large plasma currents the rotation profiles are positive and sometimes even peaked at the centre. In earlier JET experiments, the central toroidal rotation profiles were modified by varying the relative phasing of the antenna straps in the individual A2 antenna modules and the position of the ion cyclotron resonance [7]. The best overall scaling of the rotation in the core in these experiments was obtained with respect to plasma current over line averaged central electron density, as shown in [3]. However, the scattering of the data was large indicating variations due to additional variables.

That the rotation depends on the confinement in JET was reported in Ref. [2, 20], both co and counter rotation was observed in H- and L-mode. A detailed study on how the rotation profiles depend on the confinement properties of the discharge in Alcator C-Mod with H-minority heating was reported in Ref. [4]. Flat central co rotation profiles were found in EDA (enhanced D_α) H-mode plasmas [21], peaked co rotation profiles in ELM (edge localised modes) free H-modes and hollow ones in discharges with internal transport barriers. Time dependent measurements of the rotation profiles in H-modes demonstrated that rotation in the positive direction is propagating inward from the edge. It has been suggested that this propagation is anomalously fast and somewhat slower than that of the energy confinement. In L-mode both co and counter rotation was observed, although mostly rotated in the counter direction. Another interesting observation of L-mode plasmas was that the rotation in the outer part of the plasma was sensitive to the magnetic field geometry. Discharges limited on the inner wall or with lower single null had counter rotation, whereas discharges with upper single null demonstrated co rotation. Recently, mode conversion experiments in Alcator C-Mod demonstrated a relatively large co-current rotation in the core in a narrow parameter window [11].

The scaling of toroidal rotation in JET, proportional to the plasma current divided with line averaged density reported in Ref. [3], may seem to differ fundamentally from Alcator C-Mod where rotation scales with the ratio of diamagnetic energy over plasma current [13]. Note however, that contrary to the experiments on JET, the discharges in Alcator C-Mod were performed in H-mode plasmas [12-14]. In the previously mentioned JET experiments [3] at low plasma currents not only the rotation profiles were hollow, but the difference in rotation between edge and core increases in magnitude with decreasing current, which is more in line with the Alcator C-Mod scaling. However, at high plasma currents the core rotation was positive and the edge-core difference increases with plasma current contrary to the Alcator C-Mod scaling. These observations seem to indicate that rotation in the core and outer part of the plasma are driven by different mechanisms and a better approach could be to look for a scaling with respect to the difference in rotation between the edge and the core.

In order to improve the understanding of the effect of ICRF-waves on rotation, dedicated experiments were performed on JET using two ICRF heating schemes with direct electron heating

without generating fast ions: (i) ICRF mode conversion in (^{3}He)-H plasmas and (ii) ICRF heating at the second harmonic ^{3}He cyclotron resonance. Comparisons between different ICRF heating methods in similar plasmas, i.e. the same plasma current, magnetic field, plasma density and temperature, demonstrate that electron heating gives rise to a counter torque. The rotation profiles are similar as those obtained in experiments from other machines with ECRH and ohmic heating indicating that the anomalous electron transport by drift waves gives rise to a counter torque.

In this paper, the rotation measurement for the two cases will be carefully reviewed. The experimental set up is presented in section 2, the experimental results are presented in section 3, and conclusions with discussions are given in section 4.

2. EXPERIMENTAL SET UP

The experiments described in this paper were carried out with hydrogen plasmas in L-mode. ^{3}He was injected with feed back controlled gas puffing and using the method described in Refs. [22, 23]. The ^{3}He concentration was estimated from the intensity of emission lines of the various plasma constituents in the divertor with visible spectroscopy. The plasmas were heated with the JET ICRF system using the four so-called A2 antennas. Each antenna has four straps and is equipped with a Faraday screen, nearly parallel with the magnetic field, in order to reduce the coupling to slow waves. The currents in the straps can be phased relative to each other in order to change the directivity of the launched waves. Dipole phasing (i.e. relative phasing of the 4 antenna straps: $0\pi0\pi$) producing a nearly symmetric wave spectrum was used to reduce the net angular momentum of the waves.
In the experiments using mode conversion the toroidal magnetic field at the plasma center (major radius $R_0 = 2.96$m) was either 3.41T or 2.95T, the plasma current $I_p = 1.8$MA, the ICRF frequency $f = 32$MHz and the ^{3}He concentration varied between 1 and 17%. In the experiment using second harmonic ^{3}He heating $B_0 = 2.65$T, $I_p = 1.4$MA, the ICRF frequency $f = 52$MHz and the ^{3}He concentration varied from 5 to 25%.

The main diagnostic for these experiments was the active Charge exXchange Recombination Spectroscopy (CXRS) providing rotation and temperature profiles of C^{6+}, at 12 radial positions, with the innermost channel at a major radius $R = 2.88$m and the outermost channel at $R = 3.78$m. The CXRS diagnostic needs fast hydrogen or deuterium ions injected from the neutral beams for the charge exchange reaction with C^{6+}, and therefore perturbs rotation measurements. In the experiments reported here D beams were used. Since the RF-induced rotation is weak, even one beam with 2MW power will significantly affect the rotation. To reduce the perturbation only the first 50ms of short beam blips of 200ms were used and a time interval of 0.5s was left between the beam blips to relax the perturbation. The perturbation of the rotation by the beam blip can be assessed by comparing the plasma acceleration during the beam blip in 50ms intervals [3]. The uncorrected rotation at the first 50ms of the beam blip used in the graphs is close to the corrected value. Because of the relatively low rotation velocity, the rotation measurements have large relative error bars, in the order of 50%, making it difficult to make conclusions when the changes are small. The error bars were the largest for the two innermost channels therefore omitted in some of the graphs. The

measurements after application of ICRF heating showed less fluctuations. In those cases where the measured data were useable, the rotation in the outer part of the plasma was similar for the ohmic phase and the phase with ICRF-heating.

The electron temperature is measured with a 96 channel ECE radiometer system [24] measuring the electron temperature from electron cyclotron emission. The line integrated electron density was measured with the interferometer. The electron density and temperature profiles were measured with LIDAR. High-energy ions were detected using gamma emission (detected by a horizontal and vertical gamma camera) resulting from fast particle induced nuclear reactions in the plasma. In order to asses whether fast ions were produced by ICRH, energy spectra of fast neutrals leaving the plasma were measured with the Neutral Particle Analyzer (NPA).

The ion heating profiles could not be measured because of the perturbation in rotation caused by the neutral beams prohibiting measurements of the ion power deposition. The measured rotation profiles in the ohmic heating phase, before the onset of ICRF heating were often unreliable having large spatial variations. Time traces of a typical pulse are shown in Fig.1a. The ICRF-power includes modulation phases in order to determine the power deposition profiles to the electrons. The increase of the electron density and Z_{eff} with ICRF-power suggest that interaction at the antenna results in increased density containing a certain fraction of impurity ions, which is typical of these low absorption schemes [25]. Typical rotation, density and temperature profiles at the time of two beam blips are shown in Fig.1b.

3. EXPERIMENTAL RESULTS

The measured rotation in the outer part of the plasma, i.e. for major radii $R > 3.4$m, did not correlate with the ICRF-power, but seemed to vary more between different sessions than within a session. It may depend on the details of the discharge in the scrape off layer or just inside the last closed flux surfaces, due to e.g. differences in the magnetic field geometry there. Assuming that the measured rotation in the outer part of the plasma is not an instrumental offset, it has to be driven by a torque at the plasma edge, outside the first measurement points, since the angular momentum is often nearly constant in the radial range $3.4\text{m} < R < 3.78\text{m}$.

3.1 INVERTED MODE CONVERSION IN (^{3}HE)-H-PLASMAS

The power depositions for the inverted mode converted heating scenarios are expected to depend on the ICRH frequency, the magnetic field, the ratio between ^{3}He and H densities and impurities. Usually the mode converted waves are absorbed close to the mode conversion region. For mode conversion to take place the minority density has to exceed a certain threshold that depends on the temperature and parallel wave number; below this threshold cyclotron damping takes place. Compared to standard mode conversion scenarios, the inverted scenarios, have minority ion species with a smaller charge to mass ratio than the majority ion species. In these inverted mode conversion scenarios the fast wave (propagating inwards from the low field side) first tunnels through the right and left hand cut-off and then reaches the mode conversion layer where it converts to a kinetic

Alfvén wave, before encountering the minority (here ^{3}He) cyclotron layer. In previous experiments performed in H plasmas and varying the ^{3}He concentration it was shown that for inverted mode conversion scenarios the transition from ^{3}He minority heating (absorption at the minority cyclotron layer) to mode conversion heating occurs at a much lower ^{3}He concentration than in standard scenarios (~ 2% ^{3}He compared to around 10% in the standard scenarios) [26]. This was confirmed again in this set of experiments where at a ^{3}He concentration below 2% efficient ^{3}He minority heating was obtained. D ions from D beams and wall recycling and impurities, with charge to mass ratio equal to that of deuterium, lead to a second mode conversion layer between the ^{3}He cyclotron resonance layer at the centre and the D cyclotron layer on the high field side. The presence of multiple mode conversion layers and their effect on the heating efficiency as the ^{3}He concentration is increased is described in detail in [27] and can be summarised as follows: below 2-2.5% of ^{3}He efficient ^{3}He minority heating was observed, then the heating efficiency started to degrade and for ^{3}He concentrations between 4 and 6% it was difficult to couple power because one of the mode conversion layers then crossed the low field side plasma boundary. At concentrations higher than 6% the heating efficiency was fully recovered. The power deposition measured from the response of electron and ion temperatures caused by the modulation have been reported in Ref. [27]. The recovered power was typical 70% dominated by electron heating except for ^{3}He concentrations in the range 2% to 6%.

The rotation profiles for a typical JET pulse are illustrated Fig. 2. In this pulse the ^{3}He concentration was increased from 2% to 7%, the magnetic field was B_0 = 2.95T and the plasma current I_p = 1.5MA with an ICRF power of 3.6MW. The cyclotron resonance of ^{3}He was located at the high field side at about R ≈ 2.73m and the main mode conversion layer was located on the low field side of the ^{3}He cyclotron resonance. In the outer region 3.4m < R < 3.78m there is almost no change in rotation and the plasma rotates with a nearly constant angular velocity of 0.5krad/s, which also agrees within error bars with the rotation before the application of ICRF-power. This pulse shows a clear counter rotation in the core increasing with increasing ^{3}He concentration.

There is a clear difference in the rotation profiles in the core at the instant of the first beam blip at t = 6.51s and at beam blips later in the discharge. The rotation profiles at the second and third beam blip are remarkably similar. The coupled power, electron temperature and density profiles, measured with LIDAR are shown in Fig.1b. Ion temperature profiles are shown in Fig.4. All are quite similar at the time of the beam blips. Thus, the factor affecting the rotation could be the change in the ^{3}He concentration. The ^{3}He concentration, which is measured in the divertor, varies little at the time of the beam blips. The signal shows a strong increase just before the beam blip. This, however, may not be relevant for the ^{3}He concentration in the plasma core for this first beam blip, because of the time required for the ^{3}He ions to penetrate there and for the plasma to be accelerated to steady state. Note that at the last beam blip (t = 11.31s) the electron temperature was slightly lower due to a reduced ICRF power (as mentioned earlier and in [27] at ^{3}He concentrations between 4 and 6% coupling was reduced as the mode conversion layer was crossing the low field side plasma edge). At the same time the rotation profile shows a somewhat smaller central counter rotation.

The influence of the deposition profile on rotation is illustrated in Figs. 3a-e. In these figures we compare two discharges in the minority heating regime, Pulse No's: 79340 and 79345, with a low ^{3}He concentration varying from 0.5 to 1% for Pulse No: 79340 and from 0.5 to 1.5% for Pulse No: 79345. The power deposition profiles differ due to the different magnetic fields B_0 equal to 3.41T and 2.95T, respectively. In order to have similar q-profiles the plasma currents were chosen to 1.8MA and 1.5MA, respectively. The difference in magnetic field displaced the cyclotron resonance of ^{3}He in Pulse No: 79345 over 40cm towards the high field side compared to Pulse No: 79340, resulting in a less central power deposition than in the Pulse No: 79340. In order to compensate for the more off axis heating more ICRH power was applied in Pulse No: 79345, 4MW, compared to 3.4MW in Pulse No: 79340. Due to the more efficient heating, higher electron temperature and density were obtained for Pulse No: 79340. Time traces of the coupled ICRF-power, NBI blips, central temperature and averaged density are shown in Fig. 3a. The rotation profiles at t = 8.12s, t = 9.72s and t = 11.31s are shown in Fig. 3c. Since the aim of the study is to clarify the cause of the rotation we also give ion and electron temperatures and electron density profiles here shown in Fig.3b, Fig.3d and Fig.3e. (The measurements at the first blip of Pulse No: 79340 failed and have been left out). Although the power deposition profiles are different, the rotation profiles were quite similar within error bars of the order 50%. In the outer region the plasma rotates with a nearly constant angular rotation at around 2krad/s having a tendency of decreasing towards the core. Experiments with H-minority heating have revealed that the counter rotation in the centre decreases with plasma current [3]. However, there was a large spread in these data indicating that other variables were important for the rotation. For the standard mode conversion the magnitude of the core counter rotation was found to increase with power [28]. However, these discharges were performed with -90^o phasing (relative phasing of the 4 straps $0\ -\pi/2\ -\pi\ -3\pi/2$), including also a net momentum transferred to the plasma from the wave. The similarity of the rotation profiles in Fig. 3c suggests that change in rotation due to the change in plasma current is compensated by a change in electron temperature or ICRF-power. All these changes differ by 20% for the two discharges.

In Figure 4, we compare the rotation profile at the beam blip occurring at t = 6.51s for discharges Pulse No: 79350 and Pulse No: 79345. The rotation profile at this first blip differed from the rotation profile at the later beam blips. The ^{3}He concentration was below 1% for Pulse No:79345. The two discharges have the same magnetic field and plasma current but different heating power, the electron temperature and line averaged density; e.g. Pulse No: 79350 was heated with an ICRH power of 3.6MW compared to Pulse No: 79345 with 4MW, the electron temperature at the magnetic axis was 3.2keV compared to 3.0keV (see Fig.1a and Fig.3a) and the line averaged densities were $2.2\times10^{19}m^{-2}$ compared to $2.0\times10^{19}m^{-2}$. The rotation in the outer part is lower for Pulse No: 79350 than Pulse No: 79345. The difference between the rotation profiles is almost constant and equal to 2krad/s except at the innermost measurement points. The agreement between the rotation profiles (except for a certain offset) suggests that for Pulse No: 79350, the ^{3}He concentration at the first beam blip is lower than what the measurements deduced from the divertor light gives (this discrepancy was discussed in detail in [23]) or the plasma had not time enough to be close to steady state. Assuming

that the torque depends on electron heat transport by drift waves, the stronger torque caused by the higher electron temperature in Pulse No: 79345 could be compensated by the higher density to give the same rotation. This suggests that the rotation is correlated with the electron temperature rather than with the ICRF power.

Next we compare the rotation at higher ^{3}He concentrations for the discharges Pulse No's: 79350 and 79353 that had different positions for the mode conversion layer due to differences in the magnetic field. In discharge Pulse No: 79350 B_0 = 2.95T and I_p=1.5MA and the ICRF power was about 3.6MW at the three first points and 1.4MW at the last. The ^{3}He concentration increased from 2% to 7%. In discharge Pulse No:79353 B_0 = 3.41T and I_p=1.8MA. The ^{3}He concentration increased from 6% to 15%. The coupled ICRF-power, NBI blips, central temperature and averaged density are shown in Fig. 5a. The ICRF power varied as shown in Fig. 5a, and during the beam blips it was 2.4, 2.5, 3.0 and 3.5MW. The rotation profiles at t = 6.53s, t = 8.12s, t = 9.72s and t = 11.31s are shown in Fig. 5b. Fig. 5c shows the power deposition profile for direct electron heating at t = 8.9s for Pulse No:79350 (^{3}He concentration of 6%) and at t = 8.7s for Pulse No: 79353 with (^{3}He concentration of 8%). The power deposition profiles of Pulse No:79350 were more peaked in the centre compared to Pulse No:79353. Later in the discharge the ^{3}He concentration increased, and the peak of the power deposition profile in Pulse No:79353 was displaced slightly further outwards. Depending on the method of calculating the power, between 66 and 78% of the coupled power could be accounted for in Pulse No:79350 using modulation and between 82 and 90% in Pulse No:79353. However, the slightly lower power accounted for in #79350 (which had the most peaked power deposition profile) was most likely due to a lack of temperature measurements in the plasma centre. One would therefore expect that heating efficiency, fraction of absorbed power over total power, within the error bars to be similar for the two discharges.

At the two first beam blips the ICRF power was lower for Pulse No: 79353, but the temperatures and line averaged densities were similar. The angular velocity in the outer region of the plasma in Pulse No: 79353 is nearly constant and does not vary for the different beam blips as the ^{3}He concentration changes. Furthermore, the angular velocity was also similar to that in the ohmic phase. The rotation was about 1krad/s lower than for discharge Pulse No: 79350. At the first beam blip the rotation profiles were similar except for this offset. It should be noted that the discharges were done in two different sessions. The rotation at the outer part of the plasma has been seen to vary between sessions. The small difference as mentioned earlier could be due to small differences in the magnetic field geometry in the scrape off layer.

Significant counter rotation in the core was seen for Pulse No: 79350 at t = 8.12s, and at t = 9.72s and t = 11.31s and for Pulse No:79353 t = 9.72s and t = 11.31s. For Pulse No: 79350 at t = 11.31s the ICRF power tripped just before the start of the NBI heating and the electron temperature varied and therefore this point in the comparison is excluded. When comparing the rotation for Pulse No: 79350 at t = 8.12 and t = 9.72s we note that the powers and the line averaged densities were the same but the electron temperature and the rotation were both lower at t = 8.12s, indicating a scaling with electron temperature instead of power. Then we compare Pulse No:79350 at t = 9.72s with Pulse

No:79353 at t = 11.31s for which the differences in counter rotation and the electron temperatures were similar. In Pulse No: 79353 the plasma current was 20% higher, the density 5% higher and the power 10% lower with a less peaked power profile, indicating a better confinement with higher plasma current. Assuming a scaling of the rotation inversely with plasma current, one would then expect the counter rotation to be higher in Pulse No: 79350 than in Pulse No: 79353. If the power is more relevant than the electron temperature for the scaling an even larger counter rotation would then be expected in Pulse No: 79350. The difference in rotation from scaling with respect to plasma current, electron temperature or power could be an effect of mode conversion or position of the heating, but is within the error bars and can thus not be taken as a conclusive evidence of an effect of mode conversion on the rotation. We then compare the rotation for Pulse No: 79353 at t = 9.72s and t = 11.31s. The counter rotation, the power and the electron temperature was lower at t = 9.72s indicating a scaling of the rotation with either the electron temperature or the power.

3.2. SECOND HARMONIC HEATING OF ^{3}HE IN H-PLASMAS

Another set of experiments was performed in order to investigate the heating efficiency of the second harmonic heating of ^{3}He in H plasmas, a scenario investigated for the non activated phase of ITER at half field [25]. For the present study, these plasmas were very interesting as it was demonstrated that up to 15% of ^{3}He, the dominant absorption mechanism was direct electron heating via TTMP/ELD. The influence of the ^{3}He concentration in these H-plasmas is illustrated in Fig. 6. The rotation was measured at t = 11.92s in three pulses with I_p = 1.4MA and B_0 = 2.65T. The three discharges had nearly the same ICRH power, ion temperature and diamagnetic energy. Pulse No: 79361 had a ^{3}He concentration of 17% and an ICRF power of 5.2MW; Pulse No: 79362 had a ^{3}He concentration of 11% with an ICRF power of 5.5MW; and Pulse No: 79363 had a ^{3}He concentration of 8% with 5.5MW. The fraction of the ICRF power absorbed by electrons and ions depends on the ^{3}He concentration. At the highest ^{3}He concentration (as e.g. in Pulse No: 79361) the ion absorption was comparable to the electron absorption. At the lowest concentration (e.g. Pulse No: 79363) electron heating by TTMP/ELD dominates, which is consistent with the higher electron temperature obtained in such discharges. The heating efficiencies for these discharges were poor because of weak single pass damping due to the unfavourable polarisation and relative long wave lengths of the magnetosonic waves. The measured heating efficiencies at an earlier time were in the range of 25-30% [25], about half or less than that of the standard and the inverted mode conversion scenarios. The electron temperatures, the rotation and the plasma currents were about the same as for the Pulse No: 79350 with inverted mode conversion heating. The density was about 20% lower. Despite the lower heating efficiencies, these discharges showed a rather large counter rotation in the core, as shown in Fig. 8 for Pulse No: 79363. The discharge with the lowest counter rotation was Pulse No: 79361 having the lowest electron temperature, but also the highest density.

3.3 COMPARISONS OF THE ROTATION FOR DIFFERENT ICRH SCENARIOS

Common to many of the rotation profiles seen during ICRH is the nearly constant angular rotation

in the outer part of the plasma, between 3.4m < R <3.7m. When reliable data exists for the ohmic phase, before or after applying the ICRF heating, the change in rotation in the outer part is rather small. The rotation in the outer part varies between 0 and 5krad/s for different discharges, and is typically constant during several discharges or throughout the session, but can vary significantly between sessions. It is possible that the rotation in this region is sensitive to the magnetic field geometry in the scrape off layer. The outer part of the plasma is, in general co-rotating except for large magnetic field ripple [9] and some H-mode plasmas [2, 20].

There is a noticeable difference in rotation between heating scenarios involving direct absorption of the wave power by ions and those with direct absorption on the electrons even though both may result in electron heating. This difference may be caused by orbit effects of fast ions. This is illustrated by a comparison between the rotation profiles presented in section 3.1 and 3.2 and the rotation profiles for the most common heating scenario in JET, H-minority in deuterium, which at low concentrations or high powers gives rise to electron heating through fast ions. At low plasma currents, typically below 2MA, the rotation profile in the core is hollow for H-minority heating in D-plasmas [3]. Compared to the value at the boundary, the core rotates in the counter current direction. At higher currents, equal or above 2.4MA, the core rotates in the co-current direction, sometimes weakly hollow near the magnetic axis. The counter rotation increases in the core for waves launched in the counter current direction such as for -90^{o} phasing (relative phasing of the 4 straps $0\ -\pi/2\ -\pi\ -3\pi/2$) consistent with absorption of the momentum of the wave [3, 15]. The rotation profile for dipole heating is shown in Fig. 7 at $I_p = 2.4$MA, $B_0 = 2.4$T, ICRF frequency f = 42MHz, H concentration $n_H/n_D = 0.03$, and off axis heating with the cyclotron resonance intersecting the midplane at about r = 0.4m on the high field side. Fig. 7 also illustrates the difficulties to scale the core rotation: to obtain rotation profiles like the ones illustrated in Fig. 7a requires spatially alternating torques consistent with momentum transport from one region to another. Note also the increase of the co-rotation in the region between 3.35m < R< 3.55m, a phenomenon that was absent in experiments with direct electron heating. The small difference in rotation between the ohmic and the ICRF-phase suggests that the rotation in the outer region is not an ICRF-effect.

The recently reported rotation in the standard mode conversion scenario with ^{3}He in deuterium plasmas in JET [27], demonstrates a similar counter rotation in the core as the inverted mode conversion scenario. The magnitude of the core rotation increases with ICRH power and decreases with plasma current. The rotation in the plasmas heated with waves at the frequency of the second harmonic cyclotron resonance of ^{3}He in hydrogen plasmas demonstrates similar counter rotation in the core. In Fig. 8 a comparison of the rotation profiles for different heating scenarios with dominating electron heating is shown. For the Pulse No: 78847 with standard mode conversion the launched ICRF power was about half and the plasma current about twice that of the second harmonic ^{3}He in H of Pulse No: 79363. The heating in the standard mode conversion scenario (^{3}He in D plasmas) was conducted with -90^{o} (i.e $0\ -\pi/2\ -\pi\ -3\pi/2$) phasing of the antenna straps in order to increase the counter rotation by the wave momentum [27]. Although the rotation profiles are similar they have different plasma currents, ICRF-power, relative strap phasings and heating efficiencies. One can

therefore not draw any conclusion whether effects associated with mode conversion contribute to the rotation or not. However, for the discharges with the inverted mode conversion heating scheme there was no conclusive evidence that effects associated with mode conversion contributed to the rotation.

CONCLUSIONS AND DISCUSSIONS

A number of rather weak mechanisms seem to give rise to toroidal rotation of tokamak plasmas as they are heated with ICRF waves, and this makes it difficult to scale the rotation to future experiments. Some of them are intrinsic depending on transport of the momentum caused by the heating. Others are specific to the heating scenario used caused by the finite wave momentum absorbed by electrons and ions or finite orbit width effects of fast ions. Absorption of wave momentum, non-ambipolar transport by orbit effects and ripple had earlier been identified and experimentally confirmed as mechanisms causing the ICRF heated plasma to rotate toroidally. However, there are changes in the rotation profiles, for which not yet a reason has been identified. In order to separate effects caused by wide ion orbits from effects caused by heating and transport, toroidal plasma rotation was studied for scenarios with waves directly damped on the electrons. Two heating scenarios in (^{3}He)–H plasmas are used in this study: (i) inverted mode conversion for which the transition from ion minority heating to mode conversion heating takes place at lower ^{3}He concentrations than in the standard mode conversion scenarios; and (ii) heating at the second harmonic ^{3}He resonance in a hydrogen plasmas. For the inverted mode conversion scenario, the mode converted slow wave is damped by ELD at higher minority concentrations. For heating at the second harmonic ^{3}He resonance in hydrogen plasmas, with the parameters used in these experiments, the dominating absorption mechanism of the fast wave is damping on electrons by TTMP/ELD without involving mode conversion. To minimize the effect of momentum absorption by a directed wave spectrum, the experiments had been carried out with dipole (i.e. $0\ \pi\ 0\ \pi$) phasing, which gives almost toroidal symmetric wave spectra with little net toroidal momentum. The experiments were carried out with the standard low field ripple ($\delta = 0.08\%$) to avoid rotation effects caused by the ripple, which has earlier been found to give rise to counter rotation [9].

In the outer part of the plasma, between $3.4\text{m} < R < 3.75\text{m}$, the plasma "rotates" with an almost constant angular velocity for these experiments. The rotation in this region was found to vary significantly between different experimental sessions with minor changes within the sessions even when the minority concentration or the heating scenario changed. The rotation in ohmic plasmas exhibits similar rotation profiles, but with an overall lower rotation in the core [3]. When reliable measurements existed of the rotation in the ohmic phase either before or after application of RF power, the rotation in the outer part of the plasma was rather similar. The rotation in the outer part of the plasma may depend on magnetic field geometry in scrape off layer as observed in Alcator C-Mod [12]. Clear systematic changes of the rotation in this region have only been seen with increased ripple in JET [9].

In the core the plasma rotated in the counter current direction. The rotation profiles for heating

at the second harmonic ^{3}He resonance in H plasmas demonstrated similar rotation profiles as the inverted mode conversion experiments. Counter rotation in the core has earlier been seen during standard mode conversion heating with ^{3}He in D-plasmas. Thus, for these three heating methods, for which the waves were absorbed directly on electrons, and fast ion effects were negligible, the rotation profiles were similar with the counter rotation in the core scaling inversely with the plasma current. Counter rotation in the core has also been seen for minority heating in JET at low plasma current [3]. Note that this scaling does not contradict the earlier reported scaling at JET [3], which indicates that rotation increases with the plasma current, since at low plasma current the rotation was negative, i.e. counter rotating, and increasing in magnitude as the current decreased. Furthermore, when taking into account changes in the plasma current, the experiments reported here demonstrated somewhat better correlation with the temperature profile than with ICRH power, suggesting that the dominating mechanism for counter rotation in the core is related to electron heat transport rather than being a phenomenon directly related to the ICRF heating itself. Since the changes within the error bars in the rotation for the direct electron heating scenarios seem to be consistent with changes in plasma current, electron temperature and density, and since the rotation profiles for heating at the second harmonic heating of ^{3}He were similar to the discharges reported here with inverted mode conversion, there is no conclusive evidence that mode conversion in itself affects rotation for these discharges. This does not necessary contradict earlier results on Alcator C-Mod, where enhanced rotation was found in a narrow parameter region, and that effects associated with mode conversion could have contributed to the rotation in experiments at JET with standard mode conversion [26]. It should be kept in mind that because of the large relative errors of the rotation measurements at these low velocities, it is difficult to draw quantitative conclusions on the scaling because the small variations observed are almost within the capabilities of the diagnostic.

The observed counter rotation in the core surrounded by a nearly rigid rotation in the outer part of the plasma, or even absence of rotation, suggests a dipolar like torque in the core. Such a torque is expected to arise both from wave-particle interaction e.g. by drift waves in anomalous transport, where momentum is taken from one part of the plasma and given to another part of the plasma [18, 19]. Counter rotation in the core has been reported in other machines as well, using other heating methods to heat electrons such as ECRH in TCV [8] and ohmic heating in Alcator C-Mod [10]. A major difference between the rotation profile in TCV with ECRH and the rotation profile seen in JET with ICRF waves directly heating the electrons, is that in the outer part the plasma rotates with nearly constant angular momentum in JET; on the contrary, the rotation profile in TCV has a sheared rotation up to the last measured point, for which momentum is transported out of the plasma. A possible explanation of this is that rotation in the outer part of the plasma in TCV is affected by the ripple; even a modest ripple of $\delta = 1\%$ produce profiles with counter rotation at the edge in JET [9].

There is a clear difference between the difference in rotation at the core and outer region of the plasma as the concentration of ^{3}He ions changes for the inverted mode conversion experiments. The difference is lowest at the lowest concentration of the minority species, when the ions are heated

by cyclotron damping and high-energy tails are created on the ion distribution function, and the power is transferred to the electrons by collisions. A possible explanation is that in addition to the rotation caused by electron heating the rotation is influenced by ion orbit effects. Orbit effects on the rotation have earlier been identified to give a dipolar torque in JET [3].

REFERENCES

[1]. L.-G. Eriksson et al., Plasma Physics and Controlled Fusion **34** (1992) 863
[2]. L.-G. Eriksson et al., Plasma Physics and Controlled Fusion **39** (1997) 27
[3]. L.-G. Eriksson et al., Plasma Physics and Controlled Fusion **51** (2009) 044008
[4]. J.E. Rice et al., Nuclear Fusion **44** (2004) 379
[5]. L.-G. Eriksson et al., Nuclear Fusion **41** (2001) 91
[6]. S. Assas et al 2007 Radio Frequency Power in Plasmas, edited by P.M. Ryan and D.A. Rasmunsen, AIP Conference Proceedings 978 103
[7]. J. M Noterdaeme et al., Nuclear Fusion **43** (2003) 274
[8]. A. Scarabosia et al., Plasma Physics and Controlled Fusion 48 (2006) 663
[9]. M.F.F. Nave et al., Physical Review Letters **105** (2010) 105005
[10]. I. H. Hutchinson et al., Physical Review Letters 84(2000) 3330
[11]. Y. Lin et al., Physical Review Letters **101** 235002 (2008)
[12]. J.E. Rice, et al Nuclear Fusion **38** (1998) 75
[13]. J.E. Rice, et al Nucl Fusion **39** (1999) 1175
[14]. J.E. Rice, et al Nuclear Fusion **41** (2001) 277
[15]. L.-G.Eriksson et al., Physical Review Letters **92** (2004) 235001-1
[16]. J. Hedin et al., 1998 Proc. Joint Varenna- Lausanne Workshop "Theory of Fusion plasmas" (Varenna p.467, ISBN 88-7794-167-7
[17]. T. Hellsten et al., Nuclear Fusion **44** (2004) 892
[18]. T. Hellsten, 2009 Radio Frequency Power in Plasmas, edited by V. Bobokov and J.-M. Noterdaeme, AIP Conference Proceedings 1187 625
[19]. T. Hellsten, Plasma Physics and Controlled Fusion **53** (2011) 0540807
[20]. M.F.F. Nave et al., submitted to Plasma Physics and Controlled Fusion.
[21]. M. Greenwald et al., Nuclear Fusion **37** (1997)793
[22]. M. J. Mantsinen et al., Nuclear Fusion **44** (2004)33
[23]. D. Van Eester et al., Plasma Physics and Controlled Fusion **51** (2009)044007
[24]. E. de la Luna, Review of Scientific Instruments **75** (2004)3831
[25]. E. Lerche et al., submitted to Plasma Physics and Controlled Fusion
[26]. M.-L Mayoral et al, Nuclear Fusion **46** (2006) S550
[27]. D. Van Eester et al., submitted to Plasma Physics and Controlled Fusion
[28]. Y. Lin et al., submitted to Plasma Physics and Controlled Fusion

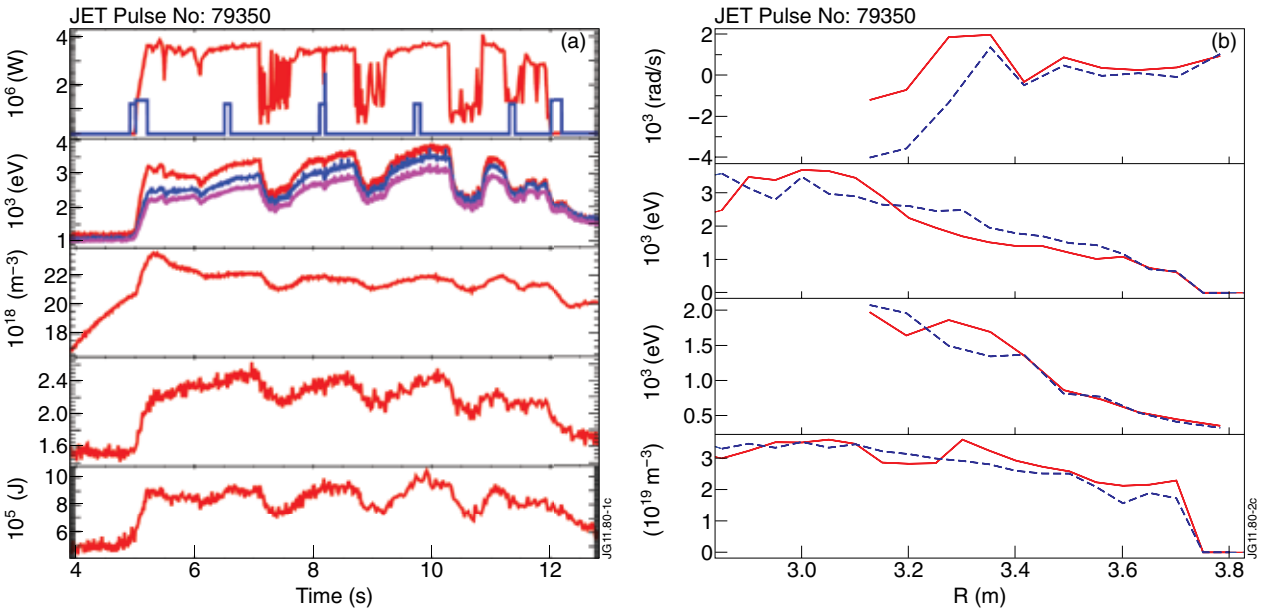

Figure 1: a) Time traces of Pulse No: 79350. RF (red) and NBI (blue) power (top graph), electron temperature (second graph) measured with the ECE radiometer at three positions, 2.95m (red), 2.75m (blue) and 2.67m (magenta). The line averaged electron density (third graph), Zeff (fourth graph) and diamagnetic energy (bottom graph).
b) Profiles of toroidal angular rotation (top graph), ion temperature (second graph), electron temperature measured with LIDAR (third graph), electron density profiles measured with LIDAR (fourth graph) all at the time of the second and fifth beam blips at t = 6.51s (red full) and t = 11.31s (blue dashed), respectively.

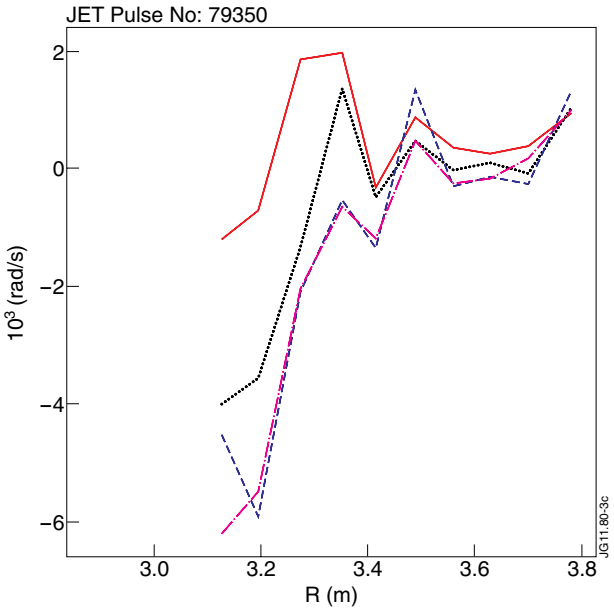

Figure 2: Toroidal angular rotation profiles for Pulse No: 79350, shown in Fig. 1a, at the time of the second beam blip at t = 6.51s (red, full line), the third blip at t = 8.12s (blue, dashed line), the forth blip at t = 9.72s (magenta, dashed dotted line) and the fifth at t = 11.31s (black, dotted line).

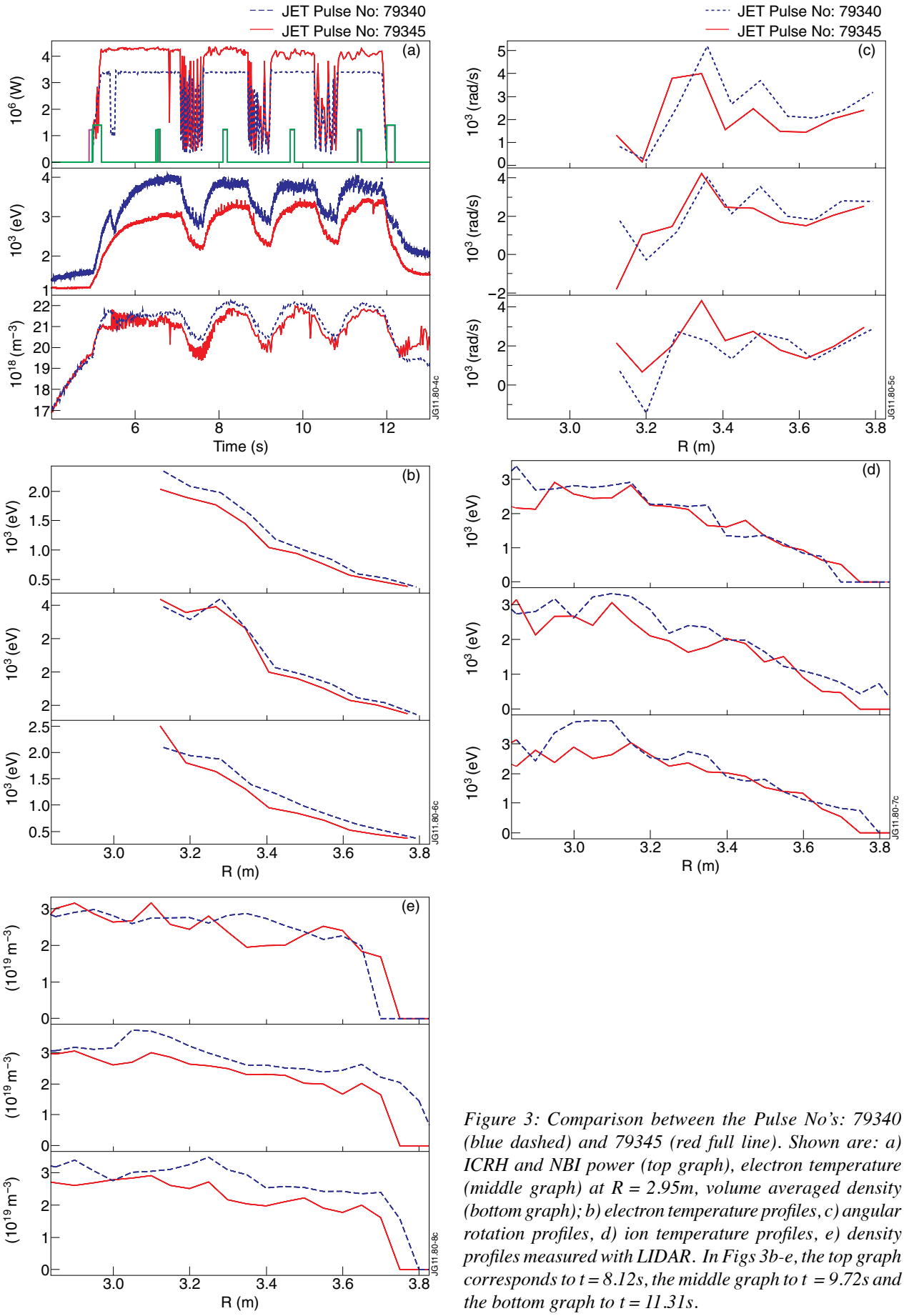

Figure 3: Comparison between the Pulse No's: 79340 (blue dashed) and 79345 (red full line). Shown are: a) ICRH and NBI power (top graph), electron temperature (middle graph) at R = 2.95m, volume averaged density (bottom graph); b) electron temperature profiles, c) angular rotation profiles, d) ion temperature profiles, e) density profiles measured with LIDAR. In Figs 3b-e, the top graph corresponds to t = 8.12s, the middle graph to t = 9.72s and the bottom graph to t = 11.31s.

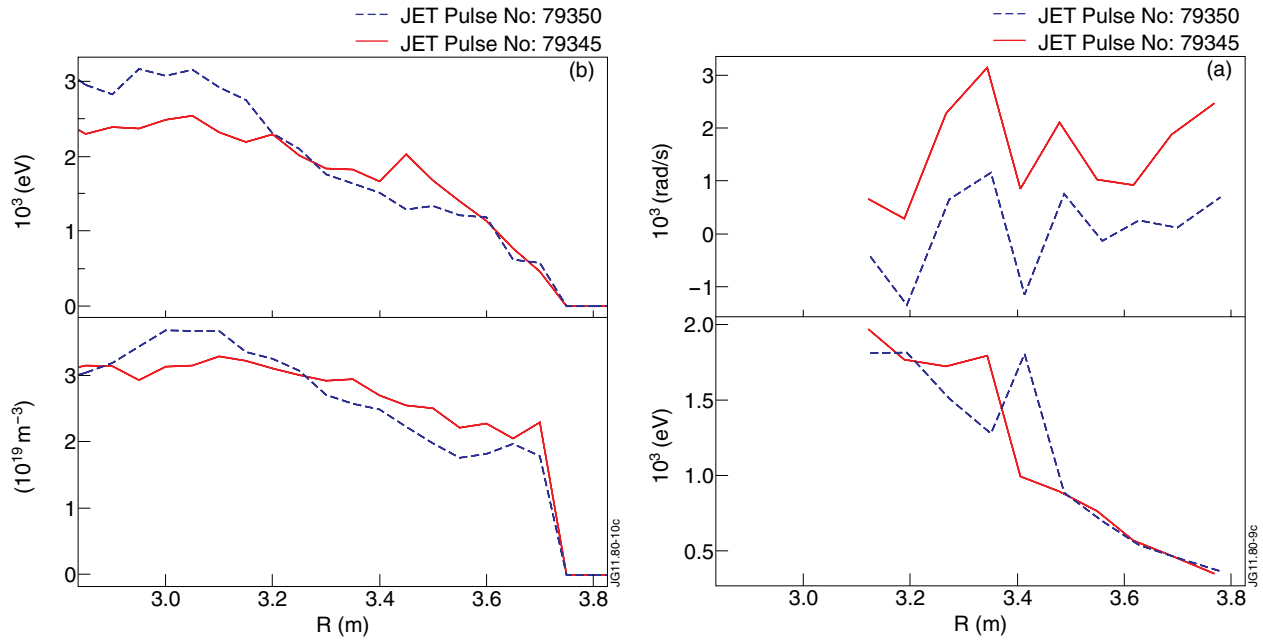

Figure 4: Comparison between various plasma profiles of Pulse No's: 79345 (red full line) and 79350 (blue dashed) at t = 6.51s. a) angular rotation (top graph) and ion temperature (bottom graph) b) electron temperature (top graph) and electron density (bottom graph) both measured with LIDAR.

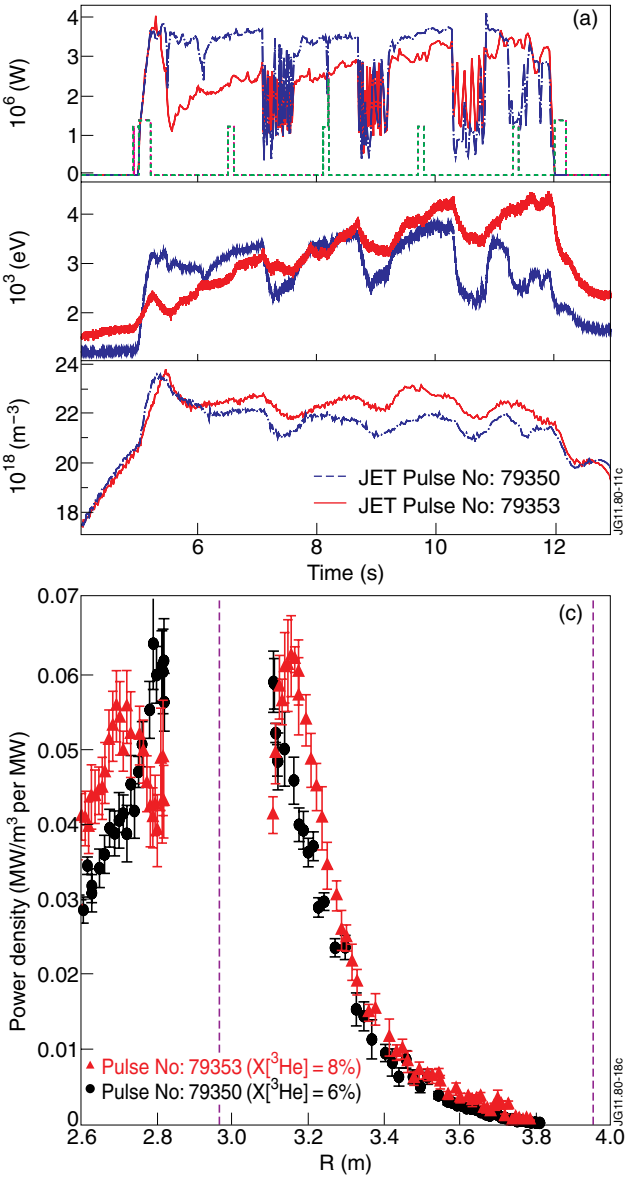

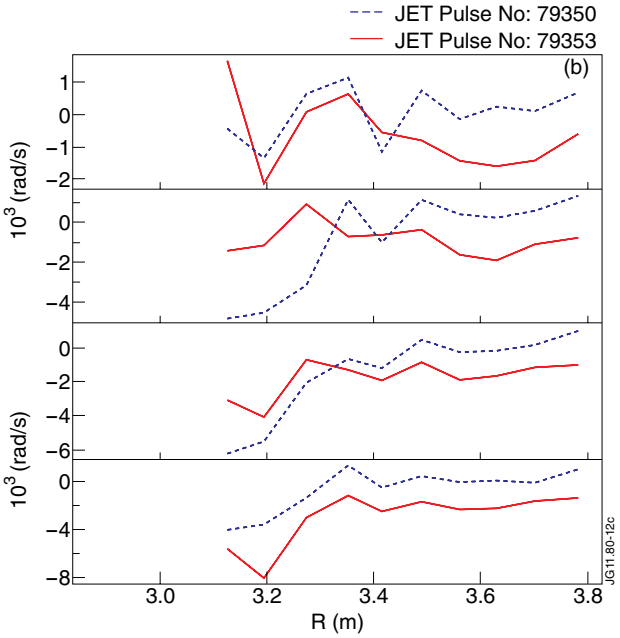

Figure 5: Comparison between the Pulse No's: 79350 (blue dashed line) and 79353 (red full line) a) ICRH and NBI power (top graph), electron temperature (middle graph) at R = 2.95m, line averaged density (bottom graph). b) Angular rotation profiles at different times from top to bottom at t = 6.51s, t = 8.12s and t = 9.72s and t = 11.31s. c) Power deposition profile normalised to coupled power of direct electron heating obtained by modulation of RF-power for discharges for Pulse No's: 79350 (black) and 79353 (red) between t = 8.7s and 8.9s, with 3He concentrations of 6% and 8%, respectively.

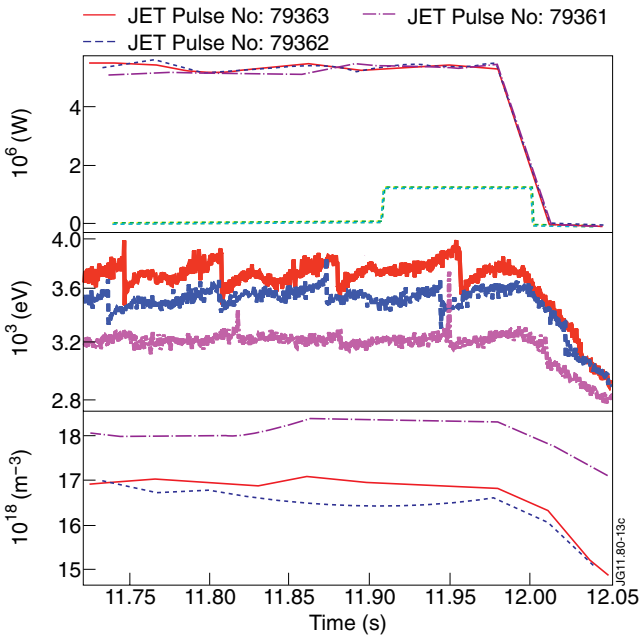

Figure 6: Comparisons between the discharges Pulse No's: 79361 (red full line), 79362 (blue dashed line) and 79363 (magenta dashed dotted line). Time traces of the discharges: ICRH and NBI power (top graph), electron temperature (middle graph) at R = 2.94m measured with ECE radiometer, volume averaged electron density (bottom graph).

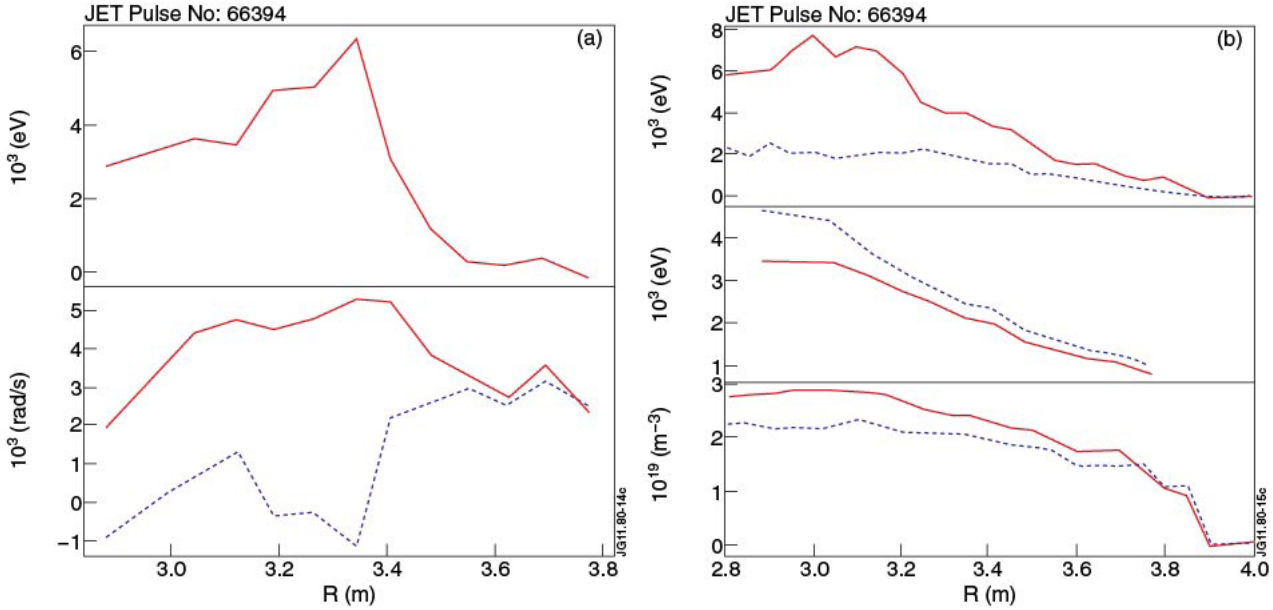

Figure 7: Rotation profiles for Pulse No: 66394 with 4.8MW hydrogen minority heating I_p = 2.4MA, B_0 = 2.4T, f = 42MHz, n_H/n_D = 0.03, off axis heating on the high field side. a) The difference between the rotation profiles at t = .03s and t = 11.53s (top graph), rotation profile at t = 7.03s during the ohmic heating phase (bottom graph , red full line) and at t = 11.53s (blue dashed line). b) Electron temperature (top graph), ion temperature (middle graph) and density profile measured with LIDAR (bottom graph).

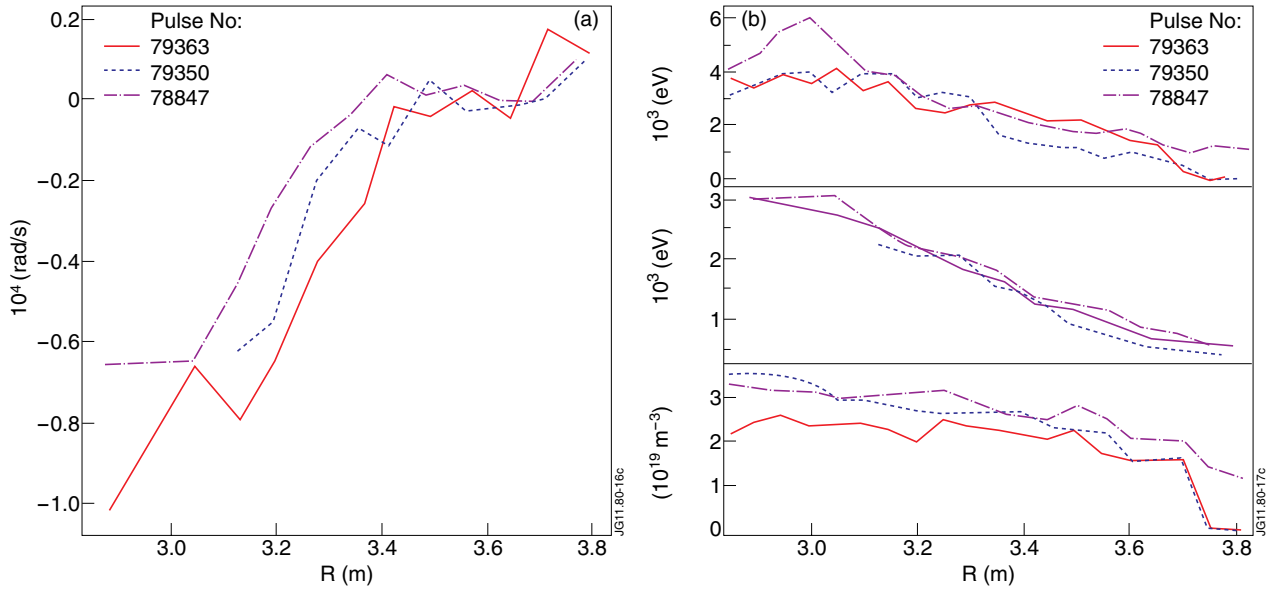

Figure 8: Comparison of the rotation profiles obtained with different heating scenarios: $\omega = 2\,\omega_{c^3He}$ (Pulse No: 79363 red full line) at t = 11.91s; inverted mode conversion at high 3He concentration (Pulse No: 79350 blue dashed line)) at t = 9.72s; standard mode conversion with high concentration and 3MW of ICRF power and −90° (i.e 0 −π/2 −π −3π/2) phasing of the four antenna straps (Pulse No: 78847 magenta dashed dotted) at t = 7.01s; a) the rotation profiles and b) the electron temperature (top graph), ion temperature (middle graph) and density (bottom graph).